(Preprint) AAS 17-608

FAMILIES OF IO-EUROPA-GANYMEDE TRIPLE CYCLERS

Sonia Hernandez*, Drew R. Jones*, and Mark Jesick*

Ballistic cycler trajectories that repeatedly encounter the Jovian moons Io, Europa, and Ganymede are investigated. The 1:2:4 orbital resonance among these moons allows for trajectories that periodically fly by the three bodies, and, in an ideal world, can repeat indefinitely. An initial search method is implemented to determine if the location of the moons in a specific geometry can give way to a possible cycler. Lambert's problem is then solved to determine the legs connecting consecutive encounters, allowing a maneuver at periapsis of the encounter if necessary. Families of solutions are classified by synodic period, and conversion to high fidelity model is outlined.

INTRODUCTION

The concept of a spacecraft periodically flying by two planets, known as cycler trajectories, has been around for decades.[1,2,3] A spacecraft on a cycler trajectory uses gravity assists to return to the starting body after a flight time commensurate with the celestial bodies' synodic period, thereby permitting indefinite repetition. The non-propulsive repeatability of these trajectories makes them of interest to human and robotic exploration applications. For example, cycler trajectories could be used for sending crew and cargo to/from Earth and Mars.[4] Inter-moon cycler trajectories for robotic tour missions could, in an ideal environment, flyby several moons for an indefinite amount of time. Russell and Strange first investigated these types of cyclers between two of Jupiter's four Galilean moons as well as around the Saturnian moons Titan and Enceladus.[5]

Triple cycler trajectories, where a spacecraft repeatedly flies by three planets or three moons have only recently been addressed. For example, cyclers that fly by Earth, Mars, and Venus can greatly reduce the hyperbolic velocity at the encounters (relative to Earth-Mars cyclers), making them more feasible for human missions.[6] Cyclers with three moons are investigated for the first time in Reference 7, designing trajectories around the Jovian system. Here, different period cyclers are considered and solutions using low-thrust in the real ephemeris are shown; however, a systematic strategy to find these trajectories is still lacking. In this paper, we focus our efforts on developing a good initial guess strategy for finding cycler trajectories around the Jovian moons Io, Europa, and Ganymede. Cyclers in this system may enable an additional tool for computing and designing tours.

The proposed strategy begins by reducing the large phase-space search through a preliminary analysis based on two-body dynamics, where geometries that can potentially allow triple cycler solutions are selected. Each potential geometry includes a sequence of close flyby encounters, and an approximate time of flight between them. Once a potential feasible geometry is chosen, a

*Mission Design and Navigation Section, Jet Propulsion Laboratory, California Institute of Technology, 4800 Oak Grove Drive, Pasadena, CA 91109. Corresponding Author: Sonia Hernandez; *Tel*: (818) 354-0418; *E-mail address*: Sonia.Hernandez-Doran@jpl.nasa.gov.

zero-radius sphere-of-influence patched conic gravity model is adopted, and Lambert's problem is solved to determine the legs connecting consecutive encounters. In this step, a velocity impulse is allowed, if needed, at periapsis of the flyby. Taking advantage of the fast computation time of solving Lambert's problem, a Monte Carlo analysis is then implemented as an optimization step, to reduce any ΔV discontinuities by searching in the vicinity of the search parameters.

The general problem of solving for a triple cycler is to find indefinitely ballistic repeatable patterns, which can only be accomplished in an ideal environment. Therefore, the aforementioned strategy is performed in an ideal ephemeris model, ensuring that exactly repeatable cyclers are found. To transition into a realistic model, a two-level approach is implemented for a specific solution. First, the ideal solution is solved via Lambert in the real ephemeris, after which a full optimization in a high-fidelity model is solved. The ballistic repeatability of the high-fidelity solution, in general, will only last for a few cycles, after which maneuvers will be required to maintain the cycler.

The paper is organized as follows. We begin by introducing some background theory on cyclers, and show how a Tisserand graph can aid in the search for these types of trajectories. The search strategy in the ideal model is then outlined, first delving into the initial guess search, followed by the Monte Carlo Lambert implementation. Several results in the ideal model are shown, with an optimized example in the real ephemeris model. Finally, conclusions and areas of future work are discussed.

BACKGROUND

The time it takes to repeat a given angular alignment of the three bodies is referred to as the synodic period T_{syn} (an extension of the two-body synodic period). The three inner Galilean moons are special in that their orbit periods exhibit what is known as a Laplace resonance,[8] that is (almost) perfect integer multiples 1:2:4. Therefore, the synodic period is one Ganymede orbit, two Europa orbits, or four Io orbits, equivalent to 7.05 days. After one synodic period, all the moons return to their initial relative configuration; however, an angular shift in their inertial location of 5.2° occurs.

A *cycle* is a portion of trajectory with flight time equal to an integer number of T_{syn}, that starts and ends at the same body, and flies by at least once through each of the bodies (Io, Europa, or Ganymede). A *cycler* trajectory is then one that completes one or more cycles. Cycler solutions are categorized into families based on the integer number of synodic periods in a cycle, and the itinerary of flybys. A cycle sequence is denoted with the first letter of each flyby body, in the order in which they are encountered, starting and ending with the same body. For example, a cycle that begins with a flyby at Europa, following a Ganymede, Io, Ganymede encounter, and ending again at Europa is denoted as EGIGE.

Understanding Triple Cyclers

To qualitatively comprehend the triple cycler trajectory, the Tisserand graph is useful.[9] These plots indicate possible gravity assist connections from a purely energy perspective (phase free). By plotting contours in v_∞ for a given body over a full range of bending angles we can visualize how different bodies may be reached and at what energy levels. A bending angle and v_∞ value map to semi-major axis and eccentricity, and therefore to any related orbital parameters such as periapsis and apoapsis radius.[10] Figure 1 presents a Tisserand graph for Io, Europa, and Ganymede. Tick marks on each contour correspond to a constant bending angle, ranging from $0 \leq \delta \leq 180°$. The v_∞ contours are in steps of 1 km/s, from $1 \leq v_\infty \leq 10$ km/s. From the graph we can observe that

Ganymede may only be reached via an Io flyby at excess speeds above 5 km/s, whereas the former may be reached via a Europa flyby at any excess speed above 2 km/s. Depending on where on the (r_a,r_p) map the spacecraft is located, multiple flybys of the same body may be necessary to move a certain distance along a countour and reach the next desired body.

Zooming into the top left corner of the Tisserand plot, a possible triple cycler path is outlined. Beginning at Europa, at a $v_\infty = 10$ km/s (orange dot), the flyby allows to intersect the Ganymede contour at a $v_\infty = 6$ km/s. A gravity assist from Ganymede (purple dot) then decreases the energy of the Jupiter centered orbit, allowing for an Io encounter at $v_\infty = 9$ km/s (blue dot), followed by a further decrease in energy to encounter Ganymede. This final flyby returns the spacecraft to the original Europa energy level, completing one cycle with sequence EGIGE.

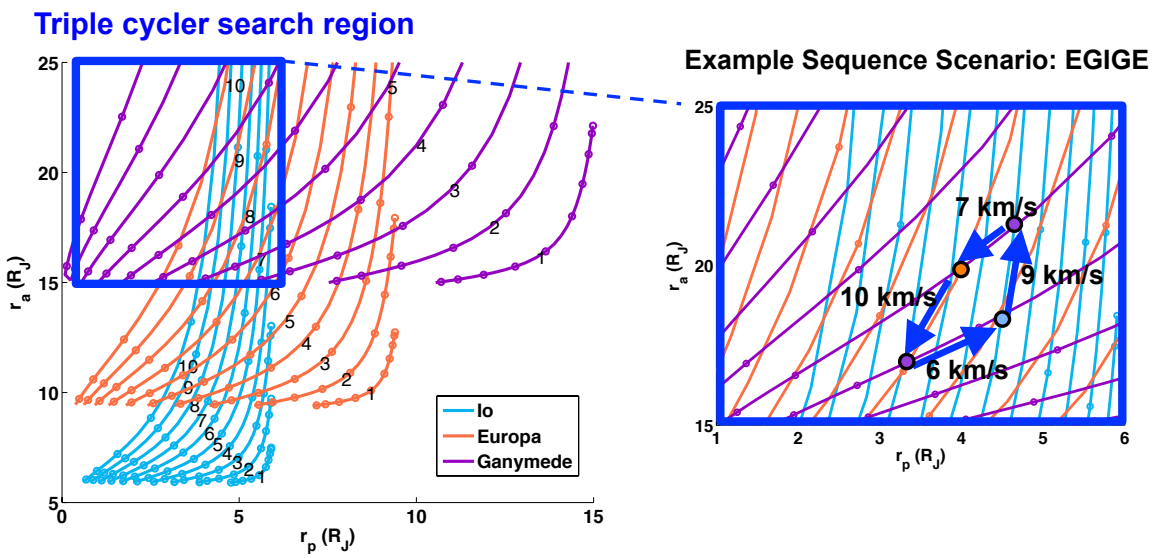

Figure 1. Tisserand plot for Io, Europa, and Ganymede. Numbers on contours represent hyperbolic excess speeds, in km/s.

Model

An approximate ephemeris is used for the initial search of cycler trajectories, where the orbits of each satellite are approximated as circular and planar, and their periods are chosen so that a perfect $\Delta = 5.2°$ displacement after each synodic period is achieved. For example, given the semi-major axis of Io, a_{Io}, the semi-major axis of Europa and Ganymede are computed as

$$a_{Eur} = \left(\frac{8\pi + \Delta}{4\pi + \Delta}\right)^{2/3} a_{Io} \quad \text{and} \quad a_{Gan} = \left(\frac{8\pi + \Delta}{2\pi + \Delta}\right)^{2/3} a_{Io}.$$

This ideal ephemeris model ensures that perfect repeating cycler trajectories can be obtained. However, the procedure outlined in this paper does not need to conform to this model, and in fact, the real ephemeris may be used, keeping in mind that cycle solutions will not in general be repeatable, and will require an extra step in the procedure to find repeatable cyclers.

METHODOLOGY

The Galilean moons have a fast revolution rate around Jupiter. For example, Io takes only 1.75 days to complete one orbit. Therefore, searching for trajectories in this system is time sensitive, since within a couple of hours Io might have moved significantly away from the planned spacecraft trajectory. Due to this sensitivity, a systematic initial guess tool is necessary to quickly search for possible cycler trajectories. Once a potential feasible solution is found, a patched conic gravity model is adopted, and Lambert's problem is solved to determine if the solution is near-ballistic with altitude flybys above the encounter body radius and below a maximum threshold.

Conic Initial Guess Tool

The initial guess search involves approximating a desired trajectory by a two-body conic, classified by three geometrical parameters: period, eccentricity, and orientation with respect to an inertial frame. The period is an integer multiple of the synodic period, the eccentricity is bounded to ensure the conic intersects all three moon orbits, and the orientation is chosen based on the location of one of the moons at the chosen departure time. The conic trajectory is searched to determine if the three flyby bodies are within a specified distance from the spacecraft when it crosses each moon's orbit. This requirement greatly reduces the search complexity for cyclers by focusing on trajectories that range $R_{Jup} \leq r_p \leq a_{Io}$ and $r_a \geq a_{Gan}$, an area outlined in the box in the Tisserand plot in Figure 1.

A cycle can repeat after n_{syn} synodic periods, where n_{syn} is a positive integer. The number of spacecraft revs for a cycle with a period $n_{syn}T_{syn}$ is driven by the constraint that the orbit must intersect all three flyby bodies in each revolution around Jupiter. Table 1 shows the possible orbit options for a cycler with synodic period ranging from 1 to 4. For example, for a 1 synodic period cycler, the period of the spacecraft can be such that it orbits Jupiter once or twice in that time period. The greyed out boxes are infeasible options since the corresponding orbits do not intersect all three bodies, and unnumbered boxes represent options that are repeated, e.g. 1:1 is equivalent to 2:2.

Table 1. Allowed search space for spacecraft revolutions around Jupiter for each synodic period

syn. per. \ s/c revs	1	2	3	4	5	6	7	8	9
1	1:1	1:2							
2	2:1	–	2:3	–	2:5				
3	3:1	3:2	–	3:4	3:5	–	3:7		
4	4:1	–	4:3	–	4:5	–	4:7	–	4:9

The initial guess search method is outlined below:

1. The semi-Major Axis a_i, directly proportional to the period $T_i = 2\pi\sqrt{a_i^3/\mu}$, is chosen from

$$n_{rev}T_i = n_{syn}T_{syn} \tag{1}$$

where n_{rev} and n_{syn} are chosen from Table 1.

2. The valid eccentricity e_i range is constrained by the maximum and minimum perijove and apojove values, such that an orbit intersects all three flyby bodies. For this system,

$$r_{p_{min}} = R_{Jup} \quad \text{and} \quad r_{p_{max}} = a_{Io}$$
$$r_{a_{min}} = a_{Gan} \quad \text{and} \quad r_{a_{max}} = \infty$$

where R_{Jup} is the mean radius of Jupiter and a_{Io} and a_{Gan} are the semi-major axis of Io and Ganymede respectively, assumed to be constant for this first stage of the search. The valid eccentricity ranges are $e_i \in [e_{min}, e_{max}]$, where e_{min} and e_{max} are computed as

$$\begin{aligned} e_{min} &= \max(1 - r_{p_{max}}/a_i, r_{a_{min}}/a_i - 1) \\ e_{max} &= \min(1 - r_{p_{min}}/a_i, r_{a_{max}}/a_i - 1) \end{aligned}$$

3. Argument of Periapsis: ω_i

For a given departure phase $\theta(t_i)$ from a specific flyby body, where $\theta(t_i) \in [0, 2\pi]$, and a chosen a_i and e_i, there are two possible orbit geometry configurations. Figure 2 shows two possible solutions for a departure from Europa at a phase θ_i (equivalent to a time t_i), with the first option departing on an outbound flyby and the second departing on an inbound flyby.

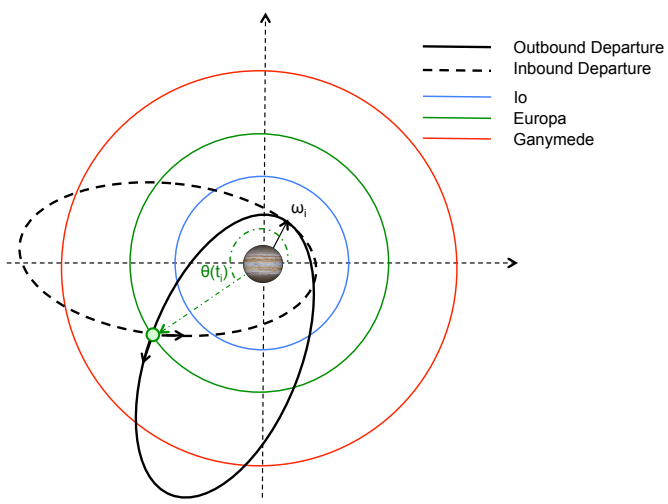

Figure 2. Possible orbit geometry configurations for departure flyby at Europa for a chosen a_i and e_i.

The three independent variables are looped over n_{rev} times, to determine if the three flyby bodies are within a specified distance from the spacecraft when it crosses each satellite's orbit. Each potential solution includes a sequence of close flyby encounters, and an approximate time of flight between them. The beauty of the initial guess algorithm is that a potential sequence of flybys is predetermined, greatly reducing the exhaustive search that would be needed otherwise due to the exponential growth of combinatory possibilities as the number of considered encounters increases.

Because the encounter body sequence of a given cycler always repeats, it does not matter which body is assigned the first flyby. For example, an EGIE cycle is equivalent to a GIEG cycle. Without loss of generality, we choose Europa as the first flyby body for any cycler and there is no need to repeat the search beginning at the other two satellites, reducing even further the search space.

Lambert Search

With the ephemeris model, the positions of each body are known for any desired time. The initial guess procedure provides a specific sequence along with the times of encounters of each body. Once both the sequence and the flyby times are defined, every pair of flybys is connected via Lambert arcs using a zero-sphere-of-influence patched conic gravity model, and allowing for a velocity impulse (ΔV) if needed at periapsis of the flyby. At this step, subsurface flybys may exist, keeping in mind all physical constraints will be added in the subsequent optimization procedure. Lambert arcs may be of the fast/slow type, and several revs are possible.[11] The number of revs in a specific arc is predefined by the time of flight between encounter bodies, and the type of arc is chosen so as to minimize the ΔV at the flyby.

Flyby Evaluation After solving Lambert's problem for adjacent legs, powered hyperbolic flybys are computed by solving for flyby altitudes. Tangential periapsis maneuvers are calculated at each encounter to account for the v_∞ mis-match.[12] Such a maneuver is often sub-optimal; however, the guess suffices for filtering poor solutions via a minimum ΔV constraint evaluation. The transfer angle is:

$$\delta = \langle \mathbf{v}_\infty^-, \mathbf{v}_\infty^+ \rangle \tag{2}$$

The periapsis radius r_p is solved iteratively via the following equation*

$$\sin^{-1}\left(\frac{\mu}{\mu + r_p {v_\infty^-}^2}\right) + \sin^{-1}\left(\frac{\mu}{\mu + r_p {v_\infty^+}^2}\right) = \delta \tag{3}$$

With r_p known, the periapsis speeds before and after the impulse are:

$$v_p^- = \sqrt{{v_\infty^-}^2 + \frac{2\mu}{r_p}} \qquad v_p^+ = \sqrt{{v_\infty^+}^2 + \frac{2\mu}{r_p}} \tag{4}$$

Since the maneuver is tangential, motion occurs in a plane containing the two asymptotes and the B-plane vector $\mathbf{B}$.[13] The two asymptotes fully define the plane (unless they are collinear). The orthogonal set of B-plane unit vectors, defined in a body-centered equatorial plane are:

$$\hat{S} = \frac{\mathbf{v}_\infty^-}{v_\infty^-} \qquad \hat{T} = \frac{(\mathbf{v}_\infty^-/v_\infty^-) \times \hat{k}}{\| \left(\mathbf{v}_\infty^-/v_\infty^-\right) \times \hat{k}\|} \qquad \hat{R} = \hat{S} \times \hat{T} \tag{5}$$

where $\hat{k} = [0, 0, 1]^T$.

The flyby bends the excess velocity vector such that the projection of $\mathbf{v}_\infty^+$ onto the B-plane is along the $-\mathbf{B}$ vector. Therefore, the angle of $\mathbf{B}$ relative to $\hat{T}$ is computed as:

$$\theta_B = \text{atan2}(\frac{\mathbf{v}_\infty^+}{v_\infty^+} \cdot \hat{R}\ ,\ \frac{\mathbf{v}_\infty^+}{v_\infty^+} \cdot \hat{T}) - \pi \tag{6}$$

Where atan2 is the quadrant specific $\arctan$ function with range $(\pi, -\pi]$. With θ_B, two periapsis states (before and after the maneuver) are formed. The states are propagated forward and backward in time from periapsis to the sphere-of-influence crossing. Luidens provides an analytical expression for the time of propagation.[14]

*This allows subsurface solutions, but those are handled by a minimum altitude constraint.

Monte Carlo Lambert Search Taking advantage of the fast computation time of solving Lambert's problem, a Monte Carlo analysis is implemented as an optimization step, to reduce any ΔV discontinuities and allow feasible flyby altitudes by searching in the vicinity of the search parameters. The flyby altitudes are constrained to lie between 25 km and 70,000 km. The search parameters are the departure phase from Europa (or chosen first body) and the times of flight between each flyby. Therefore, for a N flyby sequence cycler, there are $N-1$ search parameters, given that the total time of flight must be $n_{syn}T_{syn}$. The search parameters are allowed to vary randomly around their initial guess values, and thousands of samples are generated. Time of flight variations are of the order 10% of the flyby body period, making the range for an Io flyby about 4 hours versus 17 hours for a Ganymede flyby. These small range values are necessary due to the sensitivity of the trajectory to the fast moving system.

RESULTS

Many solutions are found in the ideal model, with synodic periods ranging from 1 to 4. Higher synodic period solutions were not searched for, because the conic search algorithm does not result in a good initial guess once the inertial shift traversed by the moons (5.2° every synodic period) becomes too large. Two examples of cycler solutions are presented.

One Synodic Period Cycler Example

A near ballistic EGIEIE cycler of the Galilean moons departing on 03-Oct-2020 ET is shown in Figure 3. This is a one synodic period trajectory, with two revolutions of the spacecraft around Jupiter. Table 3 summarizes the flyby dates, excess speeds, altitudes, and ΔV required at each flyby. The excess speeds in this example, and in general for the 1 synodic period cycler, are quite large, making them hard to fly from a navigation point of view. Figure 3(c) shows the full cycler solution, propagated for 25 synodic periods, showing how in an ideal environment, the trajectory would fly by each of the satellites indefinitely.

Table 2. Flyby summary for EGIEIE cycler departing on 03-October-2020

Flyby Body	Time of Flight (days)	Excess Speed (km/s)	Flyby Altitude (km)	ΔV (m/s)
Europa	–	12.27	9,260	1.8
Ganymede	2.03	7.29	69,990	0.1
Io	0.85	15.77	3,176	4.4
Europa	0.66	12.15	2,259	0.6
Io	2.87	15.86	494	0.0
Europa	0.65	–	–	–
Total	7.06	–	–	6.90

Four Synodic Period Cycler Example

A ballistic EGGIE cycler of the Io-Europa-Ganymede system departing on 02-Oct-2020 ET is shown in Figure 4(a), with the spacecraft range from Jupiter shown in Figure 4(b). This is a four synodic period trajectory, with five revolutions of the spacecraft around Jupiter. Figure 4(c) shows the same cycler, propagated for 16 synodic periods, showing how in an ideal environment, the trajectory would fly by the moons indefinitely. Table 3 summarizes the flyby dates, excess speeds,

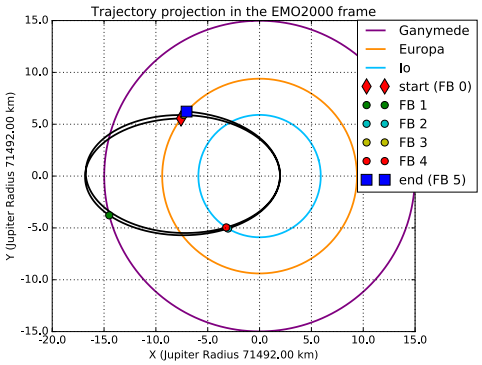

(a) Trajectory propagated for 1 repeat cycle

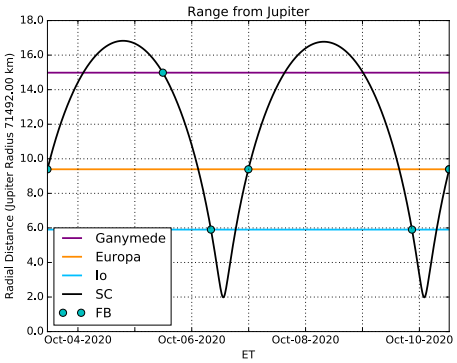

(b) Spacecraft range from Jupiter with flyby locations

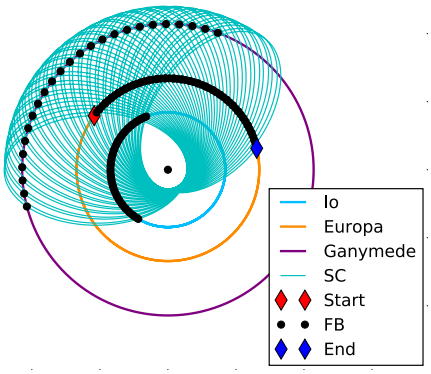

(c) Trajectory propagated for 25 repeat cycles

Figure 3. One synodic period cycler with sequence EGIEIE departing on 03-October-2020.

altitudes, and ΔV required at each flyby for one cycle. The ΔV required is 0.7 m/s, a value that can probably be optimized to zero in further optimization steps. The excess speeds for this example are much lower than for the 1 synodic period example shown above, making this type of trajectory more viable from a navigation point of view. Note how both Ganymede flybys occurs at the same value of v_∞, and, in general, for any ballistic cycler, same body encounters will occur at equal v_∞. The Tisserand plot for this flyby sequence is shown in Figure 4(d).

Table 3. Flyby summary for EGGIE cycler departing on 29-September-2020

Flyby Body	Time of Flight (days)	Excess Speed (km/s)	Flyby Altitude (km)	ΔV (m/s)
Europa	–	9.12	1,444	0.00
Ganymede	1.59	7.07	2,155	0.60
Ganymede	8.60	7.07	6,263	0.00
Io	7.34	8.38	653	0.10
Europa	10.69	–	–	–
Total	28.22	–	–	0.70

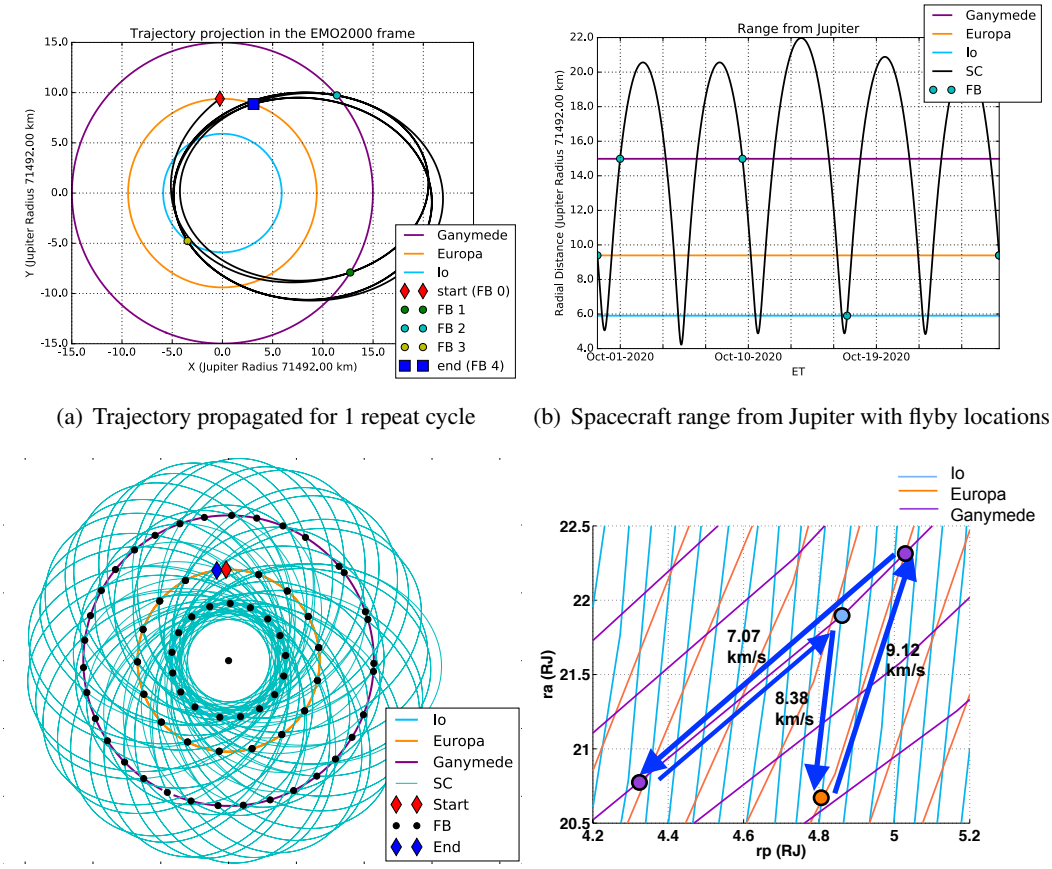

(a) Trajectory propagated for 1 repeat cycle

(b) Spacecraft range from Jupiter with flyby locations

(c) Trajectory propagated for 16 repeat cycles

(d) Tisserand Plot

Figure 4. Four synodic period cycler with sequence EGGIE departing on 02-October-2020.

For most cycler solutions found with the method described in the paper, the Jupiter-centered energy hardly varies. This is a direct consequence of the initial search method, which assumes a (constant energy) two-body conic orbit. When converting the initial guess into optimized Lambert arcs, the energy varies slightly, but still maintains the same overall initial guess structure. Visual proof of this can be observed in the Tisserand plot in Figure 4(d), where the area traversed is over a small range of r_p and r_a.

HIGH-FIDELITY SOLUTIONS

In an ideal environment, triple cycler solutions will repeat for an infinite amount of cycles. However, in the real ephemeris, the repeatability of the solution is not exact due to the fact that the relative geometry of the encounter bodies changes over time. Therefore, it is expected that in the transition from the ideal to the real model, maintenance of the cycler will be required by implementing an adaptive algorithm that can compute a new cycle at each repeat period. A two-level approach is implemented: first, the ideal solution is solved via Lambert in the real ephemeris, after which a full optimization in a high-fidelity gravity environment is solved. The ballistic repeatability of the high-fidelity solution, in general, will only last for a few cycles.

To begin the transition into the real model, the ideal solution is solved in a zero-radius sphere-of-influence patched conic gravity model via Lambert in the real ephemeris for one cycle. In general, during this step, the one cycle solution will maintain the same geometry and ballistic properties as the cycle in the ideal environment. However, when adding more cycles to the sequence, ΔV discontinuities appear, and, the geometry of the cycler begins to get distorted. This can be remedied by allowing the times of flight between each encounter to vary via the Monte Carlo Lambert search at every synodic period; however, the non-constant precession of the encounter bodies will eventually make the cycler break down.

Figure 5 shows a one synodic, one rev cycler with sequence EIGE computed in real ephemeris using Lambert arcs. The flybys occur at an altitude of 2,817 km at Io, 13,180 km at Ganymede, and 470 km at Europa. The equivalent cycler in the ideal model is ballistic, and, even though in the real ephemeris the first cycle of the solution is optimized to be ballistic, after 10 repeat cycles, the ΔV increases to almost 30 $\mathrm{m/s}$. Although hardly noticeable from Figure 5, the geometry of the cycler also changes. Conversion into a high-fidelity gravity environment is implemented for this example, and the solution remains ballistic for two cycles, after which large impulses are required to maintain the cycler.

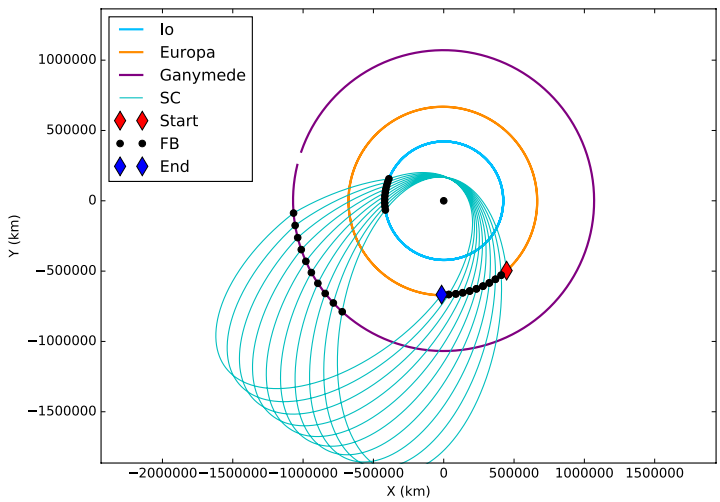

Figure 5. One synodic period cycler with sequence EIGE computed in real ephemeris for 10 repeat cycles.

CONCLUSIONS

Triple cyclers around the Jovian moons Io, Europa, and Ganymede are investigated. The 1:2:4 orbital resonance among these moons allows for trajectories that can periodically fly by the three bodies, and, in an ideal world, can repeat indefinitely, making them of potential use for robotic missions. Efforts are made on developing a good initial guess strategy, managing to reduce the large phase-space search. Once a flyby sequence is known with an initial time of flight guess between each encounter body, a zero-radius sphere-of-influence patched conic gravity model is adopted, and Lambert's problem is solved to determine the legs connecting consecutive encounters. A velocity impulse is allowed, if needed, at periapsis of the flyby. Taking advantage of the fast computation time of solving Lambert's problem, a Monte Carlo analysis is then implemented as an optimization step, to reduce any ΔV discontinuities by searching in the vicinity of the search parameters.

The initial guess search strategy is developed by approximating a desired cycler trajectory with a two-body conic orbit, and checking at what phase the encounter bodies intersect the approximated trajectory. The conic orbit must of course intersect all three flyby bodies in each revolution around Jupiter, which fixes a range of possible energies (or equivalently periapsis and apoapsis radius). Via this method, cycler trajectories are classified by two representative numbers: the integer number of synodic periods in one cycle and the integer number of revolutions around Jupiter traversed during that same amount of time.

For most cycler solutions found with the method described in the paper, the Jupiter-centered energy remains approximately constant, which is a direct consequence of assuming a two-body conic orbit during the initial search method. When converting the initial guess into optimized Lambert arcs, the energy varies slightly, but still maintains the same overall structure. Even though the initial guess search greatly reduces the search complexity, it constrains the type of cycler families that can be found to those with an almost constant energy. Therefore, future work will focus on exploring triple cyclers with more complex itineraries which combine sequences that cover a wider range of energy levels, while still maintaining the same initial guess structure.

ACKNOWLEDGMENT

This research was carried out at the Jet Propulsion Laboratory, California Institute of Technology, under a contract with the National Aeronautics and Space Administration.

© 2017. California Institute of Technology. Government sponsorship acknowledged.

REFERENCES

[1] W. M. Hollister and M. D. Menning, "Periodic swingby orbits between Earth and Venus," *Journal of Spacecraft and Rockets*, No. 7, 1970, pp. 1193–1199.

[2] D. V. Byrnes, J. Niehoff, J. M. Longuski, and B. Aldrin, "Circulating transportation orbits between Earth and Mars," *AIAA/AAS Astrodynamics Specialist Conference*, Williamsburg, VA, August 1986.

[3] D. V. Byrnes, J. M. Longuski, and B. Aldrin, "Cycler Orbit Between Earth and Mars," *Journal of Spacecraft and Rockets*, No. 30, 1993, pp. 334–336.

[4] R. P. Russell and C. A. Ocampo, "Systematic Method for Constructing Earth-Mars Cyclers Using Free-Return Trajectories," *Journal of Guidance, Control, and Dynamics*, Vol. 27, No. 3, 2004, pp. 321–335.

[5] R. P. Russell and N. J. Strange, "Planetary Moon Cycler Trajectories," *Journal of Guidance, Control, and Dynamics*, Vol. 32, No. 1, 2009, pp. 143–157.

[6] D. J. Jones, S. Hernandez, and M. Jesick, "Low Excess Speed Triple Cyclers of Venus, Earth, and Mars," *To appear in AAS/AIAA Astrodynamics Specialist Conference*, Columbia River Gorge,WA, August 2017.

[7] A. E. Lynam and J. M. Longuski, "Laplace-resonant triple-cyclers for missions to Jupiter," *Acta Astronautica*, Vol. 69, No. 3–4, 2011, pp. 158–167. doi: 10.1016/j.actaastro.2011.03.011.

[8] A. T. Sinclair, "The orbital resonance amongst the Galilean satellites of Jupiter," *Celestial Mechanics*, Vol. 12, 1975, pp. 88–96.

[9] N. J. Strange and J. M. Longuski, "Graphical Method for Gravity-Assist Trajectory Design," *Journal of Spacecraft and Rockets*, Vol. 39, No. 1, 2002.

[10] N. J. Strange, *Analytical Methods for Gravity-Assist Tour Design*. PhD thesis, Purdue University, August 2016. pp. 59-60.

[11] R. H. Battin, *An Introduction to the Mathematics and Methods of Astrodynamics*. AIAA Education Series, 1999.

[12] J. Englander, B.Conway, and T.Williams, "AutomatedMissionPlanningviaEvolutionaryAlgorithms," *Journal of Guidance, Control, and Dynamics*, Vol. 35, No. 6, 2012, pp. 1878–1887. 10.2514/1.54101.

[13] M. Jah, "Derivation of the B-Plane (Body Plane) and its Associated Parameters," tech. rep., Jet Propulsion Laboratory, 2002.

[14] R. Luidens, B. Miller, and J. Kappraff, "Jupiter High-Thrust Round-Trip Trajectories," tech. rep., NASA, 1966.